Polymer Chemistry

rsc.li/polymers

Microphase Separation

Crystalline

Amorphous

Themed issue: Polymer Chemistry Pioneering Investigators 2021

ROYAL SOCIETY OF CHEMISTRY

PAPER
Takaya Terashima *et al.*
Amphiphilic random and random block terpolymers
with PEG, octadecyl, and oleyl pendants for controlled
crystallization and microphase separation

Check for updates

Amphiphilic random and random block terpolymers with PEG, octadecyl, and oleyl pendants for controlled crystallization and microphase separation†

Sahori Imai,[a] Yasuyuki Ommura,[a] Yuki Watanabe,[b] Hiroki Ogawa,[b,c] Mikihito Takenaka, [ID][b,c] Makoto Ouchi [ID][a] and Takaya Terashima [ID] *[a]

Controlled crystallization and microphase separation of multi-component copolymers are one possibility to construct precise nanostructures in functional polymer materials. In this paper, we report the crystallization and sub-10 nm microphase separation of amphiphilic random and random block terpolymers in the solid state. By using living radical copolymerization, we designed A/B/C random terpolymers and A/C−B/C random block terpolymers, into which a hydrophobic and crystalline octadecyl group (A), a hydrophobic and amorphous oleyl group (B), and hydrophilic poly(ethylene glycol) (C) were randomly and/or site-selectively introduced as side chains. The crystallization and melting temperatures of A/B/C random terpolymers gradually decreased with increasing content of amorphous oleyl units. The random terpolymers with a relatively small amount of oleyl units induced microphase separation of the side chains to form lamellae with hydrophilic and hydrophobic alternating layers in a domain spacing of about 6 nm, while the lamellar structure was gradually disordered by increasing oleyl groups. In contrast, A/C−B/C random block terpolymers efficiently induced crystallization of the octadecyl groups even in the presence of random copolymer segments with amorphous oleyl units. The random block copolymers opened the possibility of controlling microphase separation from the side chains of the random copolymers and the main chains of the block copolymers.

Introduction

Microphase separation and self-assembly of (co)polymers[1–7] are key techniques to construct nanostructures in bulk polymers, thin films, and functional materials for applications including photolithography,[8–13] polyelectrolytes and ion conducting materials,[14–18] and solar cells.[19] Controlling nanostructures to the desired domain size and morphologies is important to design polymer materials with targeted properties and performances. The microphase separation behaviour depends on the design of immiscible segments or associating groups and the primary structures of copolymers such as degree of polymerization (DP), composition, monomer sequence (*e.g.*, block, random and alternating), and branching structures (*e.g.*, star and graft).[1–7,20] To create complex nanoscale morphologies, multi-component copolymers such as terpolymers[21–31] are more effective than common AB diblock copolymers. By designing incompatible block chains with three different A, B, and C monomers, ABC triblock copolymers[21–24] and ABC miktoarm star copolymers[25–30] induce selective self-assembly to form finely controlled and complex morphologies in the solid state, *e.g.*, core–shell gyroid,[21] sphere-in-lamellae,[25] and kaleidoscopic morphologies.[27]

Microphase separation of copolymers is driven by not only self-assembly of polymer chains but also that of side chains. In addition to the use of high χ-low N block copolymers,[6,32,33] self-assembly of polymer side chains is an alternative pathway to access sub-10 nm microphase separation structures.[34–43] By incorporating highly segregated or selectively associating or crystalline units into side chains, random[34–38] and alternating[39] copolymers and brush (co)polymers[40–43] induce self-assembly of their side chains to give ordered nanostructures in the solid state. Typically, amphiphilic random copolymers bearing hydrophilic poly(ethylene glycol) (PEG) chains and hydrophobic and crystalline octadecyl groups induce micro-

[a]Department of Polymer Chemistry, Graduate School of Engineering, Kyoto University, Katsura, Nishikyo-ku, Kyoto 615-8510, Japan.
E-mail: terashima.takaya.2e@kyoto-u.ac.jp
[b]Institute for Chemical Research, Kyoto University, Gokasho, Uji, Kyoto 611-0011, Japan
[c]RIKEN Spring-8 Center, Sayo-cho, Sayo-gun, Hyogo 679-5148, Japan
†Electronic supplementary information (ESI) available: Experimental details, SEC, DSC. See DOI: 10.1039/d0py01505a
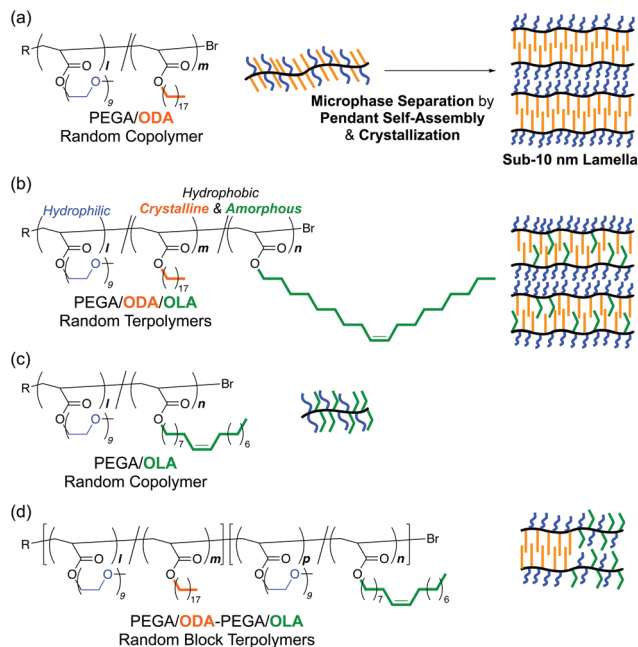
Fig. 1 Design of (a) a PEGA/ODA random copolymer (**P1**), (b) PEGA/ODA/OLA random terpolymers (**P2–P6**), (c) a PEGA/OLA random copolymer (**P7**), and (d) PEGA/ODA-PEGA/OLA random block terpolymers (**P9** and **P10**) for controlled crystallization and sub-10 nm microphase separation.

phase separation of their side chains *via* the crystallization of the octadecyl groups, forming lamellae with a domain spacing of 5–6 nm (Fig. 1a).[35] As a unique advantage of such pendant microphase separation, the domain spacing can be controlled just by the copolymer composition (*i.e.*, weight fraction of octadecyl groups); it is independent of the molecular weight and molecular weight distribution of random copolymers. Microphase separation of the amphiphilic random copolymers involves crystallization of the octadecyl groups, while whether such pendant crystallization is essential is still an unsolved matter in designing random copolymers for microphase separation.

The connection of distinct random copolymers, *i.e.*, marriage of random copolymers and block copolymers, is also one possibility to build well-ordered morphologies in self-assembled materials.[44] A/C–B/C random block copolymers potentially induce orthogonal self-assembly of the A/C random copolymer segment and the B/C counterpart. In fact, we found that A/C–B/C amphiphilic random block copolymers carrying distinct two hydrophobic groups (A: a dodecyl group, B: a benzyl group) and hydrophilic PEG side chains (C) formed double core polymers in water *via* the orthogonal folding of the A/C and B/C segments, respectively.[45] These results suggest the possibility that A/C–B/C random block copolymers undergo double microphase separation in the solid state: one is triggered by the side chains of random copolymers and the other is driven by the main chains of block copolymers. The double microphase separation may further allow us to control

the domain size of sub-10 nm microphase separation structures in dual directions of side chains and main chains.

Given these backgrounds, we herein report the crystallization and sub-10 nm microphase separation behavior of amphiphilic random or random block terpolymers in the solid state (Fig. 1). This research focused on (1) elucidating the effects of side chain crystallization on microphase separation and (2) controlling the sub-10 nm microphase separation and crystalline domains by tuning the sequence and composition of crystalline/amorphous hydrophobic units. For this, we designed A/B/C random terpolymers and A/C–B/C random block terpolymers, both of which bound a hydrophobic and crystalline octadecyl group (A), a hydrophobic and amorphous oleyl group (B), and hydrophilic PEG (C) as side chains. The amorphous oleyl group (B) consists of 18 carbons identical to the octadecyl group (A) and has the *cis*-structure of the internal olefin. The crystalline octadecyl (A) and amorphous oleyl (B) units are randomly incorporated into A/B/C random terpolymers, while these units are discretely introduced into the two blocks of A/C–B/C random block terpolymers. These terpolymers were synthesized by living radical copolymerization (Scheme 1).

The crystallization and microphase separation of their terpolymers were examined by differential scanning calorimetry (DSC), X-ray diffractometry (XRD), and small-angle X-ray scattering (SAXS). The crystallinity of A/B/C random terpolymers depended on the content of oleyl groups. The terpolymers showed broad crystallization or melting peaks of the octadecyl groups in their DSC curves, compared with random copolymers bearing PEG and octadecyl groups (no oleyl groups). The crystallization and melting temperatures decreased with increasing content of oleyl groups. The random terpolymers containing a small amount of oleyl groups formed phase-separated lamellar structures with alternating layers of hydrophilic and hydrophobic side chains, while the lamellar structures were disordered by increasing the content of oleyl
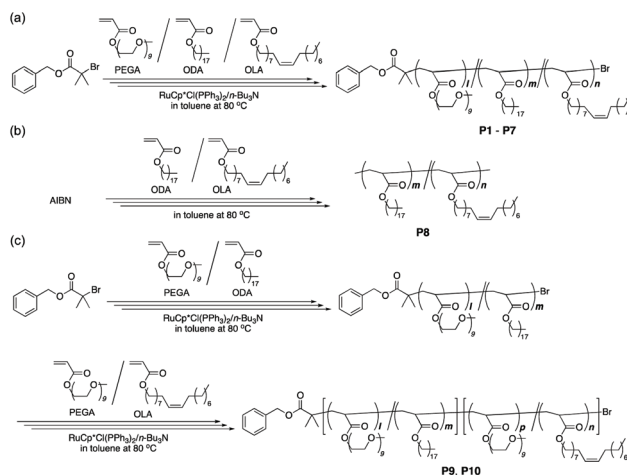
Scheme 1 Synthesis of (a) PEGA/ODA/OLA random terpolymers and PEGA/ODA or OLA random copolymers (**P1–P7**), (b) an ODA/OLA random copolymer (**P8**), and (c) PEGA/ODA-PEGA/OLA random block terpolymers (**P9** and **P10**) *via* living or free radical copolymerization.

Table 1 Synthesis of PEGA/ODA/OLA random terpolymers and related copolymers[a]

Polymer	Monomer	ODA^b (mol%)	Time (h)	Conv.[c] (%) PEGA/ODA + OLA	$M_n{}^d$ (SEC)	$M_w/M_n{}^d$ (SEC)	DP^b	$l/m/n_{obsd}{}^b$
P1	PEGA/ODA	60	47	73/74	21 400	1.26	100	40/60/0
P2	PEGA/ODA/OLA	55	71	66/64	19 100	1.35	78	31/43/4
P3	PEGA/ODA/OLA	48	160	42/42	13 900	1.19	50	20/24/6
P4	PEGA/ODA/OLA	42	160	65/64	16 600	1.28	79	32/33/14
P5	PEGA/ODA/OLA	35	214	68/64	18 100	1.60	78	31/27/20
P6	PEGA/ODA/OLA	25	160	53/55	16 900	1.27	51	20/13/18
P7	PEGA/OLA	0	214	39/39	12 500	1.36	37	14/0/23
P8	ODA/OLA	56	5	—/67	13 600	1.48	—	—

[a] **P1–P7** were synthesized by ruthenium-catalyzed living radical copolymerization: $[PEGA]_0/[ODA]_0/[OLA]_0/[BzMA-Br]_0/[RuCp*Cl(PPh_3)_2]_0/[n\text{-}Bu_3N]_0$ = 400/600/0/10/1/20 (**P1**), 400/550/50/10/1/40 (**P2**), 400/480/120/10/1/40 (**P3**), 400/420/180/10/1/40 (**P4**), 400/300/300/10/1/20 (**P5**), 400/180/420/10/1/40 (**P6**), and 400/0/600/10/1/20 (**P7**) mM in toluene at 80 °C. **P8** was prepared by free radical copolymerization: $[ODA]_0/[OLA]_0/[AIBN]_0$ = 300/300/10 mM in toluene at 80 °C. [b] ODA content (mol%), total degree of polymerization (DP), and $l/m/n$ (DP of PEGA, ODA and OLA) of the polymers determined by ^{1}H NMR. [c] Monomer conversion determined by ^{1}H NMR with tetralin as an internal standard. [d] Determined by SEC in THF with PMMA standard calibration.

groups. This indicates that the crystallization of the octadecyl groups is essential for pendant microphase separation into 5–6 nm lamellae. In contrast, A/C–B/C random block terpolymers undergo efficient crystallization of the octadecyl groups even in the presence of random copolymer chains carrying amorphous oleyl groups. Interestingly, the oleyl groups in discrete block segments hardly disturb the crystallization of octadecyl groups. As a result, the random block terpolymers opened the possibility of controlling the microphase separation of the side chains and/or block polymer chains by tuning the length (degree of polymerization) of the block segments.

Results and discussion

Synthesis of amphiphilic random or random block terpolymers

Amphiphilic A/B/C random terpolymers (**P2–P6**) bearing a hydrophilic poly(ethylene glycol) (PEG) chain (C), a hydrophobic and crystalline octadecyl group (A), and a hydrophobic and amorphous oleyl group (B) were designed to investigate the effects of an amorphous oleyl group on the crystallization and microphase separation of the side chains. As control samples, amphiphilic random copolymers carrying hydrophilic PEG and either a hydrophobic octadecyl group or a hydrophobic oleyl group (**P1** and **P7**) and a hydrophobic random copolymer bearing an octadecyl group and an oleyl group (**P8**) were prepared. To evaluate the effects of sequence distribution of octadecyl and oleyl groups on crystallization and microphase separation, amphiphilic A/C–B/C random block terpolymers comprising two random copolymers with different hydrophobic groups (**P9** and **P10**) were designed: one block segment consists of a random copolymer with PEG and crystalline octadecyl pendants and the other comprises a random copolymer with PEG and amorphous octadecyl pendants.

Amphiphilic random copolymers and terpolymers (**P1–P7**) were synthesized by ruthenium-catalyzed living radical copolymerization of PEG methyl ether acrylate (PEGA, M_n = 480, 9

average oxyethylene units), octadecyl acrylate (ODA), and oleyl acrylate (OLA) with a ruthenium catalyst $[RuCp*Cl(PPh_3)_2/n\text{-}Bu_3N]$ and a bromide initiator (benzyl 2-bromo-2-methyl-propanoate) in toluene at 80 °C (Scheme 1 and Table 1). The mole fraction of PEGA and hydrophobic monomers (ODA + OLA) was set to 40 mol% and 60 mol%, respectively. The ODA content was varied from 60 mol% to 0 mol% by changing the feed ratio of ODA and OLA, while keeping the total fraction of the hydrophobic monomers at 60 mol%.

In all the cases, PEGA and ODA and/or OLA were simultaneously consumed at the same speed, independent of the monomer feed ratio (Fig. S1†). Synchronized consumption of monomers supports the random sequence distribution of both hydrophilic and hydrophobic monomers in terpolymers and copolymers. Upon analysis by size-exclusion chromatography (SEC), the SEC curves of the products shifted to a high molecular weight with increasing monomer conversion (Fig. 2a–c and S1†). Controlled terpolymers and copolymers were obtained (**P1–P7**: M_n = 12 500–21 400, M_w/M_n = 1.19–1.60 by SEC in THF calibrated against PMMA standards). A hydrophobic random copolymer without hydrophilic PEG chains (**P8**) was prepared by free radical copolymerization of ODA and OLA with 2,2-azobis(isobutyronitrile) (AIBN) in toluene at 80 °C (M_n = 13 600, M_w/M_n = 1.48).

P1–P7 were analyzed by ^{1}H nuclear magnetic resonance (NMR) spectroscopy. As shown in Fig. 3a, **P4** indicated the proton signals of PEG chains (c: 4.4–4.2 ppm, d: 3.8–3.4 ppm, and e: 3.4–3.3 ppm) and octadecyl and/or oleyl groups (f, j: 4.2–3.8 ppm, g, k: 1.8–1.6 ppm, h, l: 1.5–1.2 ppm, m: 2.1–2.0 ppm, n: 5.5–5.3 ppm, and j, o: 1.0–0.8 ppm), in addition to those of polyacrylate backbones (a, b) and the initiator benzyl ester fragment (p: 5.2–5.0 ppm, Ph group: 7.5–7.3 ppm). In **P7**, the area ratio of the oleyl olefin protons (n) agreed with that of the other methylene and methyl protons (j, k, o, etc.), meaning that the pendant olefin is intact during copolymerization (Fig. 3b). The direct introduction of the oleyl groups into copolymer side chains without side reactions and gelation was also confirmed by free radical copolymerization of ODA and OLA and ^{1}H NMR analysis of the
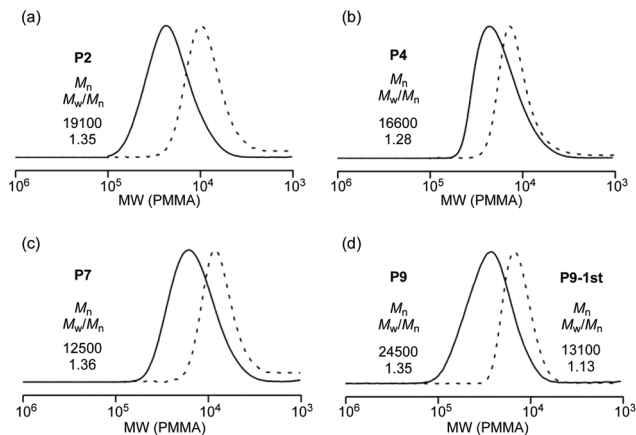
Fig. 2 SEC curves of (a) **P2**, (b) **P4**, (c) **P7**, their intermediates obtained at earlier conversion (dashed lines, PEGA/ODA + OLA conversion = (a) 16%/16%, (b) 20%/21%, and (c) 12%/12%), and (d) **P9** and **P9-1st** (macroinitiator, dashed line).
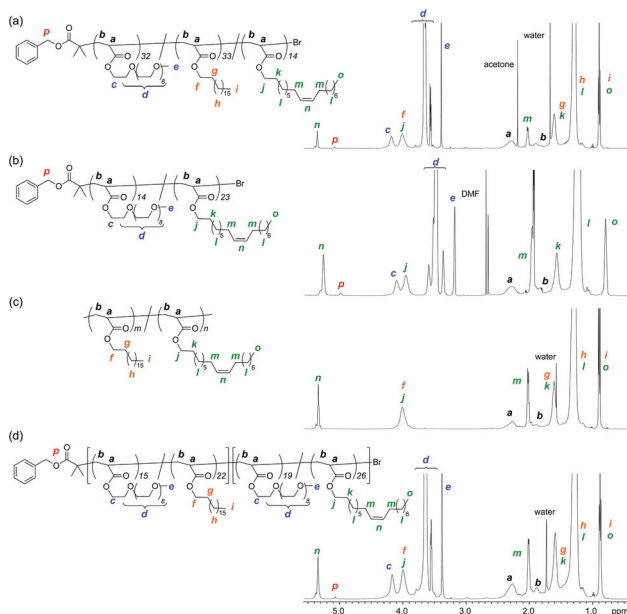

Fig. 3 ^{1}H NMR spectra of (a) **P4**, (b) **P7**, (c) **P8**, and (d) **P9** in CDCl$_3$ at 25 °C.

resulting **P8** (Fig. 3c). The total degree of polymerization (DP) and composition (PEGA/ODA/OLA = $l/m/n$) of **P1–P7** were determined by ^{1}H NMR from the area ratio of the respective side chain units to the initiator fragment (Table 1). The $l/m/n$ values were close to those calculated from the feed ratio of the monomers to the initiator and their monomer conversions.

Amphiphilic random block terpolymers (**P9** and **P10**) were prepared by ruthenium-catalyzed living radical copolymerization of PEGA and OLA with bromine-capped PEGA/ODA random copolymers and a ruthenium catalyst (Scheme 1c). Here, two PEGA/ODA random copolymers with different DPs were employed as macroinitiators to control the length of the

crystalline 1st block segments against that of amorphous 2nd block segments. Well-controlled PEGA/ODA random copolymers were obtained from ruthenium-catalyzed living radical copolymerization of PEGA and ODA with benzyl 2-bromo-2-methyl-propanoate as an initiator (**P9-1st**: M_n = 13 100, M_w/M_n = 1.13, DP = 37, **P10-1st**: M_n = 19 900, M_w/M_n = 1.18, DP = 79, Table 2). Then, the random copolymers were applied to copolymerization of PEGA and OLA with RuCp*Cl(PPh$_3$)$_2$/n-Bu$_3$N in toluene at 80 °C, resulting in well-controlled random block terpolymers (**P9**: M_n = 24 500, M_w/M_n = 1.35, **P10**: M_n = 29 000, M_w/M_n = 1.39, Table 2, Fig. 2d and S1†). The DP and composition (PEGA/ODA-PEGA/OLA = l/m–p/n) of **P9** and **P10** were determined by ^{1}H NMR (Table 2 and Fig. 3d).

Crystallization and microphase separation of random terpolymers

Effects of oleyl groups on crystallization. PEGA/ODA/OLA random terpolymers (**P2–P6**), a PEGA/ODA random copolymer (**P1**), and a PEGA/OLA random copolymer (**P7**) were analyzed by differential scanning calorimetry (DSC) to examine the effects of oleyl pendants on the crystallization. The bulk polymer samples were obtained from the evaporation of CH$_2$Cl$_2$ solutions of their polymers at room temperature, followed by drying under reduced pressure. DSC measurements of the polymer samples were then conducted by the following heating and cooling processes: the samples were first heated from 40 °C to 150 °C to erase the thermal history. Then, the samples were cooled to −80 °C and subsequently heated to 150 °C. The heating and cooling rates were 10 °C min^{-1} and −10 °C min^{-1}, respectively. The first cooling and second heating processes are shown in Fig. 4a and b, respectively.

A PEGA/ODA random copolymer (**P1**) sharply showed an exothermic signal originating from the crystallization of the octadecyl groups in the cooling process (crystallization temperature: T_c = 38.5 °C) and an endothermic signal stemming from the melting of the octadecyl groups in the heating process (melting temperature: T_m = 43.0 °C) (Table 3). In contrast, a PEGA/ODA/OLA (40/42/18 mol%) random terpolymer (**P4**) indicates the broad exothermic and endothermic signals of the octadecyl groups in the cooling and heating processes, respectively (Fig. 4a and b). Both T_c and T_m of **P4** were lower than those of **P1**; the enthalpy of crystallization and melting for **P4** was also smaller than the corresponding enthalpy for **P1** (Table 3). Similarly, broad exothermic and endothermic signals with lower T_c and T_m were observed in an ODA/OLA random copolymer (**P8**) (Fig. S2 and S3†). These results importantly suggest that oleyl groups incorporated into **P4** affect the crystalline domains of the octadecyl groups in the solid state.

To investigate the crystallization dependent on oleyl groups in detail, random terpolymers with different ODA/OLA contents (ODA/OLA = 55/5–25/35 mol%, **P2–P6**) were evaluated. All the samples showed both exothermic and endothermic signals in cooling and heating processes, while the peak broadness, T_c, T_m, and enthalpy of crystallization and melting were dependent on the ODA/OLA ratio (Fig. 4a and b). Both exothermic and endothermic signals gradually broadened with increasing

Table 2 Synthesis of PEGA/ODA-PEGA/OLA random block copolymers[a]

Polymer	Monomer	ODA/OLA[b] (mol%)	Time (h)	Conv.[c] (%) PEGA/ODA or OLA	$M_n{}^d$ (SEC)	$M_w/M_n{}^d$ (SEC)	DP[b]	$l/m–p/n_{obsd}{}^b$
P9-1st	PEGA/ODA	59/0	7	26/27	13 100	1.13	37	15/22
P9	PEGA/OLA	27/32	79	23/28	24 500	1.35	82	15/22–19/26
P10-1st	PEGA/ODA	59/0	7	43/43	19 900	1.18	79	32/47
P10	PEGA/OLA	43/17	45	28/27	29 000	1.39	109	32/47–12/18

[a] Random block copolymers were synthesized by ruthenium-catalyzed living radical copolymerization. **P9-1st**: $[PEGA]_0/[ODA]_0/[BzMA-Br]_0/[RuCp*Cl(PPh_3)_2]_0/[n-Bu_3N]_0 = 400/600/10/1/40$ mM in toluene at 80 °C. **P9**: $[PEGA]_0/[OLA]_0/[\textbf{P9-1st}]_0/[RuCp*Cl(PPh_3)_2]_0/[n-Bu_3N]_0 = 560/840/10/1/40$ mM in toluene at 80 °C. **P10-1st**: $[PEGA]_0/[ODA]_0/[BzMA-Br]_0/[RuCp*Cl(PPh_3)_2]_0/[n-Bu_3N]_0 = 640/960/10/1/20$ mM in toluene at 80 °C. **P10**: $[PEGA]_0/[OLA]_0/[\textbf{P10-1st}]_0/[RuCp*Cl(PPh_3)_2]_0/[n-Bu_3N]_0 = 560/840/10/1/20$ mM in toluene at 80 °C. [b] Hydrophobic monomer content (mol%) in the respective block segments, total degree of polymerization (DP), and $l/m–p/n$ (DP of PEGA/ODA-PEGA/OLA) of the random (block) copolymers determined by ^{1}H NMR. [c] Monomer conversion determined by ^{1}H NMR with tetralin as an internal standard. [d] Determined by SEC in THF with PMMA standard calibration.
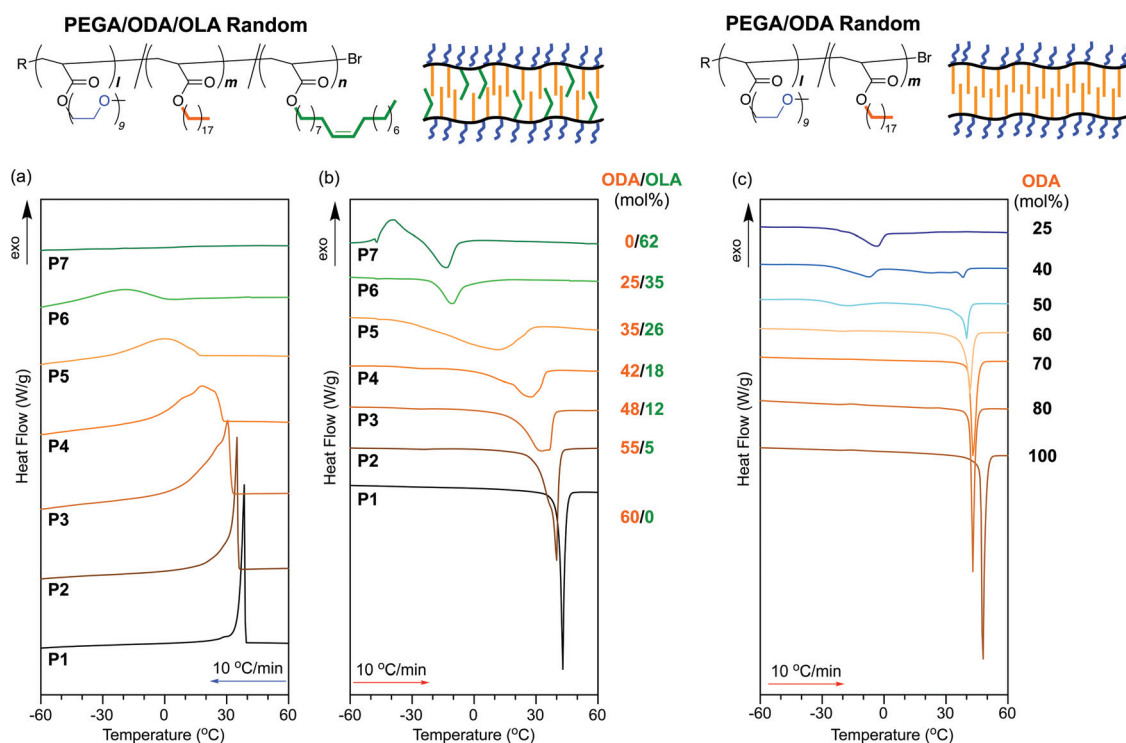
Fig. 4 DSC curves recorded for (a) the first cooling scans and (b and c) second heating scans of (a and b) PEGA/ODA/OLA random copolymers (**P1–P7**: ODA + OLA = 60 mol%) and (c) PEGA/ODA random copolymers (ODA = 25–100%)[35] between −80 °C and 150 °C. The cooling and heating rates were −10 °C min⁻¹ and 10 °C min⁻¹, respectively.

amorphous OLA units. T_c, T_m, and enthalpy of crystallization and melting decreased with increasing OLA units. **P5** with 35 mol% ODA exhibited a quite broad endothermic peak from −30 to 30 °C (T_m = 11.0 °C). **P6** with 25 mol% ODA, as well as a PEGA/OLA random copolymer (**P7**), exhibited exothermic and endothermic signals at temperatures lower than 0 °C (Table 3). The crystallization and melting peaks would be derived from PEG side chains and/or trace water included in the samples (*e.g.*, intermediate water).[46]

In contrast, PEGA/ODA random copolymers with different ODA contents (40–80 mol%) maintained the sharp endothermic signals originating from the melting of the octadecyl groups (Fig. 4c).[35] T_m of the random copolymers did not so

decrease with decreasing ODA mole fraction, different from that of **P2–P5** with oleyl groups (Fig. 5a). These results suggest that the broadness of exothermic or endothermic signals and decreasing T_c and T_m in **P2–P5** are attributed to the decreasing size of crystalline domains by the sequence distribution of octadecyl units and oleyl units. Since a PEGA/ODA random copolymer with 25 mol% ODA did not show a melting peak of the octadecyl groups, random copolymers and terpolymers containing octadecyl units less than 25 mol% hardly induce crystallization of the octadecyl groups.

The enthalpy of melting for **P2–P4** and PEGA/ODA random copolymers (with over 40 mol% ODA) was linearly proportional to the ODA content (Fig. 5b), namely, the melting enthalpy

Table 3 Crystallization behavior of PEGA/ODA/OLA terpolymers and related copolymers

Entry	Polymer	Monomer	ODA (mol%)	$T_c{}^a$ (°C)	$\Delta H_c{}^a$ (J g^{-1})	$T_m{}^a$ (°C)	$\Delta H_m{}^a$ (J g^{-1})
1	**P1**	PEGA/ODA	60	38.5	52.2	43.0	52.2
2	**P2**	PEGA/ODA/OLA	55	35.0	50.5	39.9	50.3
3	**P3**	PEGA/ODA/OLA	48	30.5	44.5	32.9	43.6
4	**P4**	PEGA/ODA/OLA	42	18.6	34.2	27.4	34.2
5	**P5**	PEGA/ODA/OLA	35	−0.6	27.9	11.0	27.3
6	**P6**	PEGA/ODA/OLA	25	−21.4	16.4	−10.3	16.4
7	**P7**	PEGA/OLA	0	−39.1^b	18.4^b	−13.2	18.4
8	**P8**	ODA/OLA	56	13.6	35.3	23.9	35.1
9	**P9**	PEGA/ODA-PEGA/OLA	27	−33.9^b	3.8^b	−16.3	3.3
				35.6	23.0	40.7	22.8
10	**P10**	PEGA/ODA-PEGA/OLA	43	38.2	37.3	42.7	37.9
11	**P1 + P7**	PEGA/ODA + PEGA/OLA	60	−37.4^b	9.1^b	−12.2	9.2
				35.4	27.1	44.0	25.1

^{a} The samples of entries 1–11 were analyzed by DSC between the temperature range of −80 °C and 150 °C. The cooling and heating rates were 10 °C min^{-1} and −10 °C min^{-1}, respectively. The crystallization temperature (T_c) and the enthalpy of crystallization (ΔH_c) were obtained from the first cooling scans of the samples from 150 °C. The melting temperature (T_m) and the enthalpy of melting (ΔH_m) were obtained from the second heating scans of the samples from −80 °C. ^{b} The crystallization temperature (T_c) and the enthalpy of crystallization (ΔH_c) were obtained from the second heating scans of the samples from −80 °C.
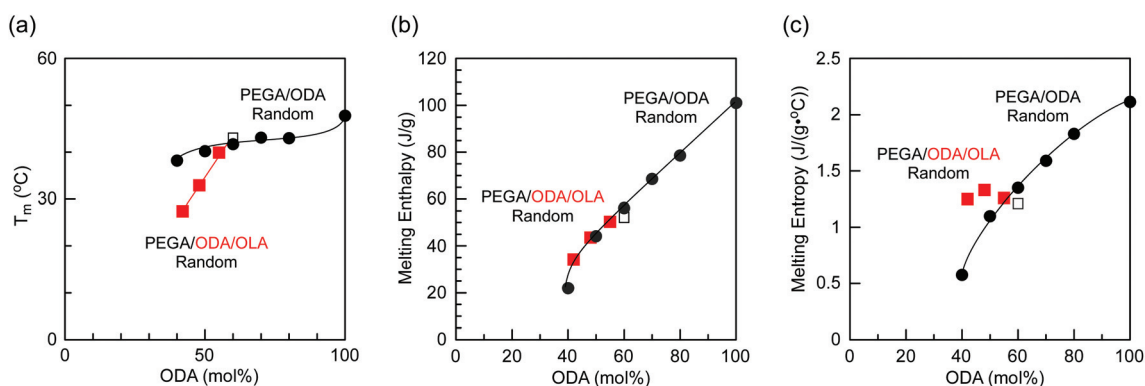
Fig. 5 (a) Melting temperatures and (b) enthalpy and (c) entropy of melting of octadecyl groups in PEGA/ODA/OLA random terpolymers (red squares: **P2**, **P3**, and **P4**) and PEGA/ODA random copolymers (black circles,[35] black open square: **P1**) as a function of the ODA content (mol%).

normalized by the ODA content was constant. This suggests that the octadecyl groups in **P2**–**P4** have crystalline structures similar to those in PEGA/ODA random copolymers. The entropy of melting for **P2**–**P4** was also calculated with the following: $\Delta S_m = \Delta H_m/T_m$. The entropy values for **P2**–**P4** were almost identical, although those for PEGA/ODA random copolymers decreased with decreasing ODA content (Fig. 5c). The entropy of melting is generally related to volume and conformation changes of polymers through phase transition from a crystalline state to a melting state. Thus, this result implies that **P2**–**P4** with 60 mol% hydrophobic content form similar self-assembled nanostructures in the solid state.

Crystalline structures. **P1**, **P2** and **P5** were analyzed by X-ray diffractometry (XRD) at 20 °C. **P1** and **P2** with over 55 mol% ODA showed sharp peaks at 21.6° of 2θ (Fig. 6a), indicative of the formation of the hexagonally packed structure of the octadecyl pendants in d = 4.1 Å.[35] This is consistent with their melting temperatures being higher than the analysis temperature. Additionally, sharp peaks were detected at a small angle area at around 3° of 2θ. This suggests the formation of longi-

tudinal nanostructures derived from the microphase separation of the side chain groups. In contrast, **P5** with 35 mol% ODA only showed amorphous halo peaks at around 20° of 2θ owing to the low melting temperature (T_m = 11.0 °C).

Temperature-dependent XRD of **P2** was conducted between 20 and 50 °C. Upon heating the sample from 20 °C to 40 °C, the height of the sharp peak at 21.6° decreased and an amorphous halo peak gradually overlapped with the sharp peak. At 50 °C, the sharp peak completely disappeared, meaning that the octadecyl groups were disordered. Upon cooling from 50 °C to 20 °C, the octadecyl groups crystallized to show a sharp peak at 21.6° of 2θ. These results indicate that the octadecyl groups of **P2** reversibly form a hexagonally packed structure through melting and crystallization processes. It should also be noted that small peaks at around 3° of 2θ were also reversibly observed in this heating and cooling process, suggesting the reversible formation of longitudinal nanostructures.

Effects of oleyl groups on microphase separation. To evaluate microphase separation, **P2**, **P3**, **P4**, **P5**, and **P6** were analyzed by small angle X-ray scattering (SAXS) at 25 °C, compared

Fig. 6 (a) X-ray diffractograms of (a) **P1**, **P2**, and **P5** at 20 °C and (b) temperature-dependent X-ray diffractograms of **P2** at 20, 30, 40 and 50 °C and 20 °C after cooling from 50 °C. (c) SAXS profiles of **P1**, **P2**, **P3**, **P4**, **P5**, **P6**, and **P7** at 25 °C.

Fig. 7 (a) DSC curves recorded for the second heating scans of **P1**, **P7**, **P9**, **P10** and the binary blend of **P1** and **P7** from −80 °C to 150 °C with a heating rate of 10 °C min^{-1}. (b) SAXS profiles of **P1**, **P9**, **P10** and the binary blend of **P1** and **P7** at 25 °C. (c) Enthalpy of melting of PEGA/ODA random copolymers (black circles),[35] PEGA/ODA/OLA random terpolymers (**P2**, **P3**, and **P4**: gray squares), **P9** (red square), **P10** (blue square) and the binary blend of **P1** and **P7** (orange open square) as a function of the ODA content (mol%).

with a PEGA/ODA random copolymer (**P1**) and a PEGA/OLA random copolymer (**P7**) (Fig. 6c). **P1** and **P2** with 55 mol% ODA exhibited integer order peaks (1 : 2 : 3) to form lamellar structures. The domain spacing of **P1** and **P2** was estimated as 5.2 nm and 5.5 nm from the peaks at q = 1.20 nm^{-1} and 1.14 nm^{-1}, respectively. Considering the size range, the lamellar structure is derived from the microphase separation of PEG side chains and octadecyl and oleyl groups.[35] In contrast, **P5**, **P6**, and **P7** only showed broad peaks at around q = 1 and 2.5 nm^{-1}. In addition to such broad peaks, **P3** and **P4** showed small integer order peaks (1 : 2), where the domain spacing was 5.6 nm. The broad peaks in **P3**, **P4**, and **P5** are attributed to the disordered state *via* partial or complete melting of octadecyl groups at the SAXS measurement temperature. This is consistent with the melting temperature of the samples. In other words, this result importantly demonstrates that the crystallization of the octadecyl groups is essential for the formation of longitudinal lamellar structures *via* the microphase separation of random copolymer side chains. In **P1**, **P2**, **P3**, and **P4**, the domain spacing ranged between 5.2 nm and 5.6 nm. The small difference of the domain spacing implies that oleyl groups with the *cis* conformation affect the interdigitating and/or end-to-end structures of octadecyl groups in their crystalline domains.[42]

Crystallization and microphase separation of random block terpolymers

The crystallization and microphase separation of PEGA/ODA-PEGA/OLA random block terpolymers (**P9** and **P10**) were

evaluated by DSC and SAXS (Fig. 7). Upon analysis by DSC, **P9** and **P10** showed sharp endothermic signals derived from the melting of the octadecyl groups in the heating process (T_m = 40.7, 42.7 °C), as well as **P1** as a model polymer for the 1st block segments (Fig. 7a). The binary blend of **P1** and **P7** also showed a similar melting peak at 44.0 °C. The melting peak for octadecyl groups of **P9** comprising a short crystalline block exhibited a shoulder at the low temperature region. In **P9**, **P10** and the binary blend of **P1** and **P7**, the enthalpy of melting was proportional to the mole fraction of ODA, although these samples have a relatively low total ODA content below 40 mol% (Fig. 7c). These results indicate that octadecyl groups of random copolymers efficiently induce crystallization even in the presence of random copolymers bearing amorphous oleyl groups.

P9, **P10** and the binary blend of **P1** and **P7** were analyzed by SAXS, compared with **P1**. **P10** with a long crystalline 1st block and the binary blend of **P1** and **P7**, as well as **P1**, showed integer order peaks (1 : 2 : 3) stemming from lamellar structures (Fig. 7b). The domain spacing of **P10** (d = 5.4 nm) and the binary blend (d = 5.2 nm) was close to that of **P1** (d = 5.2 nm). It is interesting that **P1** still induces microphase separation into lamellae even in the presence of **P7** bearing amorphous oleyl groups. In contrast, **P9** with a short crystalline 1st block indicated not only a peak derived from the microphase separation of the side chains at q = 1.14 nm^{-1} (d = 5.5 nm) but also another peak at q = 0.50 nm^{-1} whose domain spacing was

calculated to be 13 nm (Fig. 7b), although the former microphase separation of the side chains does not give longitudinal structures.

These results suggest that the random block terpolymers competitively induce microphase separation of the side chains and block polymer chains, dependent on the length and/or volume fraction of the 1st and 2nd block segments. Lamellar microphase separation of the crystalline octadecyl groups and PEG chains in the presence of amorphous oleyl-bearing copolymers requires relatively long 1st crystalline random segments. **P9** induces double microphase separation in the solid state: one originates from the side chains of hydrophilic PEG and crystalline octadecyl groups in the 1st random segment and the other is probably derived from microphase separation between the crystalline 1st block domains and the amorphous 2nd block domains.[47] Since **P10** with a long crystalline 1st block did not show such a low q peak, the volume fraction of two blocks would also affect the double microphase separation behaviour. To understand these microphase separation behaviour and morphologies, detailed analyses are now under investigation using various random block copolymers with different chain lengths, compositions, and side chains. These interesting discoveries would open new possibilities to three-dimensional control of nanodomain structures and sizes within solid polymer materials.

Conclusions

In summary, we designed amphiphilic random and random block terpolymers bearing PEG chains, crystalline octadecyl groups, and amorphous oleyl groups to examine the crystallization and microphase separation behaviour. Dual incorporation of octadecyl and oleyl groups as hydrophobic side chains opened the possibility to control not only the crystallization and melting temperatures but also temperature-dependent microphase separation and the crystalline domain sizes and structures in the solid state. In particular, we found the possibility that random block terpolymers comprising a crystalline random segment and an amorphous counterpart induced double microphase separation in different size scales stemming from side chains and polymer chains. The volume fractions of crystalline and amorphous blocks also affected the microphase separation behaviour and longitudinal lamellar structures. Therefore, the controlled crystallization and microphase separation systems using amphiphilic random and random block terpolymers would bring innovation to construct well-defined nanostructures in polymer materials that are potentially applicable to various research fields including nanotechnologies and photolithography.

Conflicts of interest

There are no conflicts to declare.

Acknowledgements

Notes and references

1 A. J. Meuler, M. A. Hillmyer and F. S. Bates, *Macromolecules*, 2009, **42**, 7221–7250.
2 H.-C. Kim, S.-M. Park and W. D. Hinsberg, *Chem. Rev.*, 2010, **110**, 146–177.
3 J. K. Kim, S. Y. Yang, Y. Lee and Y. Kim, *Prog. Polym. Sci.*, 2010, **35**, 1325–1349.
4 Y. Mai and A. Eisenberg, *Chem. Soc. Rev.*, 2012, **41**, 5969–5985.
5 A. H. Gröschel and A. H. E. Müller, *Nanoscale*, 2015, **7**, 11841–11876.
6 C. Sinturel, F. S. Bates and M. A. Hillmyer, *ACS Macro Lett.*, 2015, **4**, 1044–1050.
7 C. M. Bates and F. S. Bates, *Macromolecules*, 2017, **50**, 3–22.
8 C. M. Bates, M. J. Maher, D. W. Janes, C. J. Ellison and C. G. Willson, *Macromolecules*, 2014, **47**, 2–12.
9 M. Park, C. Harrison, P. M. Chaikin, R. A. Register and D. H. Adamson, *Science*, 1997, **276**, 1401–1404.
10 P. Mansky, C. K. Harrison, P. M. Chaikin, R. A. Register and N. Yao, *Appl. Phys. Lett.*, 1996, **68**, 2586–2588.
11 R. A. Segalman, *Mater. Sci. Eng., R*, 2005, **48**, 191–226.
12 C. Park, J. Yoon and E. L. Thomas, *Polymer*, 2003, **44**, 6725–6760.
13 W. J. Durand, G. Blachut, M. J. Maher, S. Sirard, S. Tein, M. C. Carlson, Y. Asano, S. X. Zhou, A. P. Lane, C. M. Bates, C. J. Ellison and C. G. Willson, *J. Polym. Sci., Part A: Polym. Chem.*, 2015, **53**, 344–352.
14 W.-S. Young, W.-F. Kuan and T. H. Epps, *J. Polym. Sci., Part B: Polym. Phys.*, 2014, **52**, 1–16.
15 C. E. Sing, J. W. Zwanikken and M. O. de la Cruz, *Nat. Mater.*, 2014, **13**, 694–698.
16 R. L. Weber, Y. Ye, A. L. Schmitt, S. M. Banik, Y. A. Elabd and M. K. Mahanthappa, *Macromolecules*, 2011, **44**, 5727–5735.
17 M. W. Schulze, L. D. McIntosh, M. A. Hillmyer and T. P. Lodge, *Nano Lett.*, 2014, **14**, 122–126.
18 Y. Ye, J.-H. Choi, K. I. Winey and Y. A. Elabd, *Macromolecules*, 2012, **45**, 7027–7035.
19 P. D. Topham, A. J. Parnell and R. C. Hiorns, *J. Polym. Sci., Part B: Polym. Phys.*, 2011, **49**, 1131–1156.
20 M. W. Matsen, *Macromolecules*, 2012, **45**, 2161–2165.

21 T. A. Shefelbine, M. E. Vigild, M. W. Matsen, D. A. Hajduk, M. A. Hillmyer, E. L. Cussler and F. S. Bates, *J. Am. Chem. Soc.*, 1999, **121**, 8457–8465.

22 T. S. Bailey, H. D. Pham and F. S. Bates, *Macromolecules*, 2001, **34**, 6994–7008.

23 J. Chatterjee, S. Jain and F. S. Bates, *Macromolecules*, 2007, **40**, 2882–2896.

24 A. Guliyeva, M. Vayer, F. Warmont, A. Takano, Y. Matsushita and C. Sinturel, *Macromolecules*, 2019, **52**, 6641–6648.

25 K. Hayashida, N. Saito, S. Arai, A. Takano, N. Tanaka and Y. Matsushita, *Macromolecules*, 2007, **40**, 3695–3699.

26 A. T. Lorenzo, A. J. Müller, M.-C. Lin, H.-L. Chen, U.-S. Jeng, D. Priftis, M. Pitsikalis and N. Hadjichristidis, *Macromolecules*, 2009, **42**, 8353–8364.

27 Y. Matsushita, K. Hayashida, T. Dotera and A. Takano, *J. Phys.: Condens. Matter*, 2011, **23**, 284111, 1–12.

28 A. Nunns, C. A. Ross and I. Manners, *Macromolecules*, 2013, **46**, 2628–2635.

29 Y. Rho, C. Kim, T. Higashihara, S. Jin, J. Jung, T. J. Shin, A. Hirao and M. Ree, *ACS Macro Lett.*, 2013, **2**, 849–855.

30 T. Higashihara, S. Ito, S. Fukuta, S. Miyane, Y. Ochiai, T. Ishizone, M. Ueda and A. Hirao, *ACS Macro Lett.*, 2016, **5**, 631–635.

31 J. Masuda, A. Takano, J. Suzuki, Y. Nagata, A. Noro, K. Hayashida and Y. Matsushita, *Macromolecules*, 2007, **40**, 4023–4027.

32 J. G. Kennemur, L. Yao, F. S. Bates and M. A. Hillmyer, *Macromolecules*, 2014, **47**, 1411–1418.

33 T. Isono, N. Kawakami, K. Watanabe, K. Yoshida, I. Otsuka, H. Mamiya, H. Ito, T. Yamamoto, K. Tajima, R. Borsali and T. Satoh, *Polym. Chem.*, 2019, **10**, 1119–1129.

34 D. Neugebauer, M. Theis, T. Pakula, G. Wegner and K. Matyjaszewski, *Macromolecules*, 2006, **39**, 584–593.

35 G. Hattori, M. Takenaka, M. Sawamoto and T. Terashima, *J. Am. Chem. Soc.*, 2018, **140**, 8376–8379.

36 K. Matsunaga, K. Tanaka and J. Matsui, *Chem. Lett.*, 2018, **47**, 500–502.

37 E. Barnard, R. Pfukwa, J. Maiz, A. J. Muller and B. Klumperman, *Macromolecules*, 2020, **53**, 1585–1595.

38 R. Imanishi, Y. Nagashima, K. Takishima, M. Hara, S. Nagano and T. Seki, *Macromolecules*, 2020, **53**, 1942–1949.

39 S. Mete, K. G. Goswami, E. Ksendzov, S. V. Kostjuk and P. De, *Polym. Chem.*, 2019, **10**, 6588–6599.

40 M. Matsumoto, M. Takenaka, M. Sawamoto and T. Terashima, *Polym. Chem.*, 2019, **10**, 4954–4961.

41 K. Ebata, Y. Hashimoto, K. Ebara, M. Tsukamoto, S. Yamamoto, M. Mitsuishi, S. Nagano and J. Matsui, *Polym. Chem.*, 2019, **10**, 835–842.

42 K. Ebata, Y. Hashimoto, S. Yamamoto, M. Mitsuishi, S. Nagano and J. Matsui, *Macromolecules*, 2019, **52**, 9773–9780.

43 Y. Kimura, M. Takenaka, M. Ouchi and T. Terashima, *Macromolecules*, 2020, **53**, 4942–4951.

44 J. D. Quinn and R. A. Register, *J. Polym. Sci., Part B: Polym. Phys.*, 2009, **47**, 2106–2113.

45 M. Matsumoto, T. Terashima, K. Matsumoto, M. Takenaka and M. Sawamoto, *J. Am. Chem. Soc.*, 2017, **139**, 7164–7167.

46 M. Tanaka, T. Motomura, N. Ishii, K. Shimura, M. Onishi, A. Mochizuki and T. Hatakeyama, *Polym. Int.*, 2000, **49**, 1709–1713.

47 M. Xiang, D. Lyu, Y. Qin, R. Chen, L. Liu and Y. Men, *Polymer*, 2020, **210**, 123034.